

# Fermi liquid breakdown and evidence for superconductivity in $\text{YFe}_2\text{Ge}_2$

Y. Zou,<sup>1</sup> Z. Feng,<sup>1,\*</sup> P. W. Logg,<sup>1</sup> J. Chen,<sup>1</sup> G. I. Lampronti,<sup>2</sup> and F. M. Grosche<sup>1</sup>

<sup>1</sup>*Cavendish Laboratory, University of Cambridge, J J Thomson Ave, Cambridge CB3 0HE, UK*

<sup>2</sup>*Dept. of Earth Sciences, University of Cambridge, Downing Street, Cambridge CB2 3EQ*

(Dated: February 24, 2019)

The paramagnetic d-electron system  $\text{YFe}_2\text{Ge}_2$  displays an unusually high Sommerfeld ratio of the specific heat capacity  $C/T \sim 100 \text{ mJ/molK}^2$  at low temperature and can be tuned to the border of spin density wave order by partial substitution of Y with isoelectronic Lu, suggesting that  $\text{YFe}_2\text{Ge}_2$  is located close to a spin density wave quantum critical point. Our ambient pressure, low temperature measurements reveal signatures of Fermi liquid breakdown such as an increasing  $C/T$  on cooling and a  $3/2$  power law temperature dependence of the electrical resistivity. Moreover, samples of  $\text{YFe}_2\text{Ge}_2$  with high residual resistance ratios display full superconducting transitions below  $T_c \simeq 1.8 \text{ K}$  in the electrical resistivity and up to 80% Meissner volume fraction in DC magnetisation measurements.

The investigation of quantum critical phenomena associated with incipient antiferromagnetic or spin density wave order in transition metal compounds has been held back by the scarcity of candidate systems in this class of materials.  $\text{LuFe}_2\text{Ge}_2$  crystallizes in the well known  $\text{ThCr}_2\text{Si}_2$  type structure ( $I4/mmm$ ) and has been reported to exhibit spin density wave order below 9 K [1, 2]. In the spin density wave state, the Fe moments align ferromagnetically in the basal plane and couple antiferromagnetically to their nearest neighbours in the crystallographic  $c$  direction. In  $\text{LuFe}_2\text{Ge}_2$  the transition temperature increases with increasing pressure [3], which makes it difficult to approach the quantum critical point in this material. Here, we concentrate on its sister compound  $\text{YFe}_2\text{Ge}_2$ , which is paramagnetic at ambient pressure [1]. Recent measurements on the substitution series  $(\text{Y/Lu})\text{Fe}_2\text{Ge}_2$  [4] demonstrated that antiferromagnetic order occurs on the Lu-rich side of the series, with  $\text{Lu}_{0.8}\text{Y}_{0.2}\text{Fe}_2\text{Ge}_2$  as the critical composition.

We have grown high quality crystals of  $\text{YFe}_2\text{Ge}_2$  from tin flux, following the recipes given in [1]. We have also grown polycrystals by radio frequency melting of the elements (Y 3N, Fe 4N, Ge 6N) on a water-cooled copper boat, followed by annealing in vacuum at  $800^\circ \text{C}$  for 7 days. The residual resistivity ratios (RRR =  $\rho(300 \text{ K})/\rho(2 \text{ K})$ ) obtained from flux growth were typically about 10, whereas annealed polycrystals reached resistivity ratios up to 50. The electrical resistivity and the magnetic susceptibility were measured in an ADR to below 0.1 K, and the specific heat capacity was measured on a Physical Properties Measurement System (PPMS) with a  $^3\text{He}$  insert to below 0.4 K. The magnetisation data was acquired in a Cryogenic SQUID magnetometer with a  $^3\text{He}$  insert to below 0.3 K. X-ray studies confirmed the quality and composition of our samples, giving the lattice parameters  $a = 3.964(6) \text{ \AA}$ ,  $c = 10.457(4) \text{ \AA}$  and the conventional unit cell volume  $V = 164.37(2) \text{ \AA}^3$ . Our samples were found to be at least 99% phase pure, and the only impurity phase which could be identified in some of the samples is a ferromagnetic Fe/Ge alloy.

At elevated temperatures  $T > 2 \text{ K}$ , our findings are

consistent with those reported previously [1]: The magnetic susceptibility is small and weakly temperature dependent, whereas the Sommerfeld coefficient of the specific heat capacity,  $C/T$  is surprisingly high, reaching values near  $\simeq 90 \text{ mJ/molK}^2$  at 2 K (Fig. 1). Extending the measurements to lower  $T$  reveals a further increase of  $C/T$  (Fig. 1).

The electrical resistivity is metallic (inset Fig. 1) but displays an unusual power-law temperature dependence

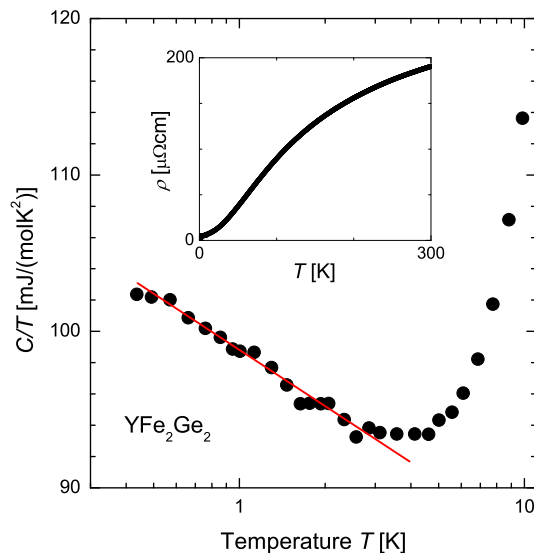


FIG. 1. Sommerfeld ratio of the specific heat capacity,  $C/T$ , vs. temperature  $T$  in rf-furnace grown polycrystalline  $\text{YFe}_2\text{Ge}_2$ . The Sommerfeld ratio rises with decreasing temperature  $T < 4 \text{ K}$  and reaches about  $100 \text{ mJ}/(\text{molK}^2)$ . More detailed, lower temperature data will be required to distinguish between a logarithmic  $T$ -dependence or the  $\gamma_0 - a\sqrt{T}$  form predicted near a 3D spin density wave quantum critical point. The inset shows the electrical resistivity of  $\text{YFe}_2\text{Ge}_2$  at elevated temperatures.

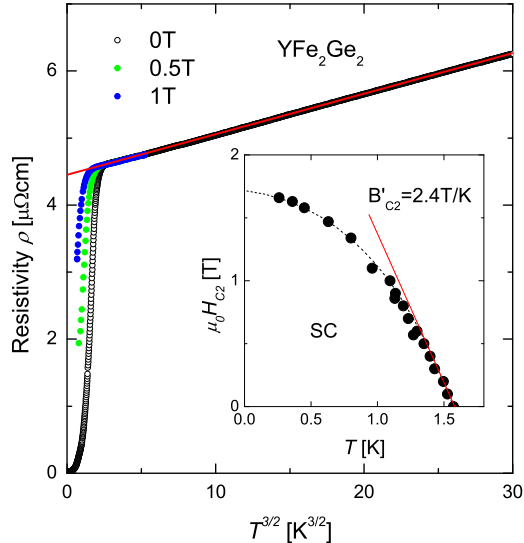


FIG. 2. Resistivity of rf-induction furnace grown polycrystalline  $\text{YFe}_2\text{Ge}_2$ , showing full resistive superconducting transitions at  $T < 1.8$  K and  $T^{3/2}$  temperature dependence in the normal state resistivity. The suppression of  $T_c$  in applied magnetic fields yields an initial slope  $B'_{c2} \simeq 2.4$  T/K (inset) and an extrapolated zero-temperature critical field of  $H_{c2} = 1.7$  T.

of the form  $\rho(T) \simeq \rho_0 + AT^{3/2}$  up to temperatures of the order of 10 K (Fig. 2).

This anomalous power-law temperature dependence in the electrical resistivity points towards proximity to a quantum critical point, whereas the weak  $T$ -dependence of the magnetic susceptibility appears to rule out a major role for ferromagnetic spin fluctuations. This suggests that  $\text{YFe}_2\text{Ge}_2$  is positioned close to an antiferromagnetic (or spin density wave) quantum critical point, which is consistent with the finding that partial substitution of Y by Lu indeed induces spin density wave order [4]. In the absence of mass enhancement connected to correlated f-bands, the strongly enhanced Sommerfeld coefficient (band structure prediction based on Wien2k [5]:  $8 \text{ mJ/molK}^2$ ) must then be attributed to the effects of nearly critical antiferromagnetic fluctuations, presumably centred on the ordering wavevector reported from neutron scattering studies,  $\mathbf{Q} = (001)$  [3].

Below 2 K, superconducting transitions are apparent in the electrical resistivity (Fig. 2) as well as in the DC magnetisation (Fig. 3). While the onset of the resistive transition is observed at  $T_c^{\rho} \simeq 1.8$  K, the onset of superconductivity is apparent in DC magnetisation measurements only below  $T_c^{\text{mag}} \simeq 1.5$  K. This and the fact that the diamagnetic signal does not saturate entirely down to 280 mK suggests that  $T_c$  varies across the sample. For the sample shown, the superconducting volume fraction

extracted from the Meissner effect (Fig. 3) amounts to at least 80%.

Comparing polycrystals with different residual resistance ratio, we find a clear correlation between sample purity and both the size of the superconducting jump and the value of  $T_c$  observed in resistivity measurements. Full superconducting transitions are obtained in the purest polycrystalline samples, with  $\text{RRR} \simeq 30\text{--}50$ , while unannealed polycrystals with lower RRR as well as the flux-grown single crystals with  $\text{RRR} \simeq 10$  only show partial transitions.

Heat capacity measurements down to 400 mK have not revealed a clear anomaly associated with the superconducting transition. This could be attributed to the broad nature of the transition, as evident from the magnetisation data. Heat capacity measurements to lower temperature are in preparation.

The initial slope of the resistive upper critical field is  $dB_{c2}/dT \simeq -2.4$  T/K (inset of Fig. 2). This results in a clean-limit weak-coupling orbital-limited critical field  $B_{c2}^{(o)} \simeq -0.73 T_c dB_{c2}/dT \simeq 2.8$  T [6]. This value significantly exceeds the observed critical field in the low temperature limit of  $\simeq 1.7$  T, suggesting that the low temperature critical field is Pauli limited. In the standard treatment (e.g. [7]), the extrapolated orbital-limited critical field corresponds to a superconducting co-

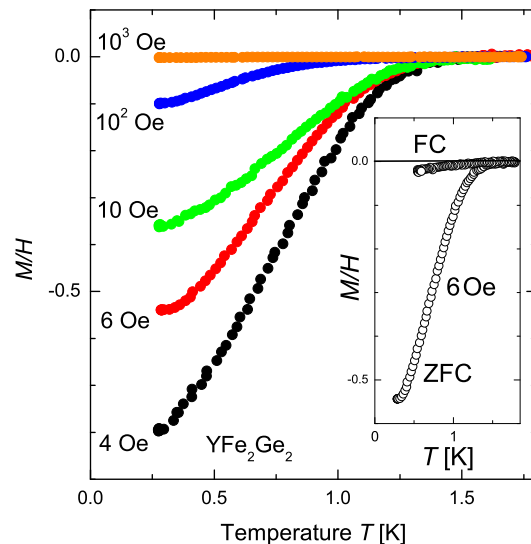


FIG. 3. The diamagnetic signal, which is observed in the DC magnetisation below 1.5 K, is illustrated above. The size and position of the diamagnetic signature shifts with increasing magnetic field, leading to a lower critical field of the order of 2 mT. The inset shows the difference between the zero-field cooled and the field cooled magnetic response.

herence length  $\xi_0 = \left[ \Phi_0 / \left( 2\pi B_{c2}^{(o)} \right) \right]^{1/2} \simeq 108 \text{ \AA}$ , where  $\Phi_0 = h/(2e)$  is the quantum of flux. Such a short coherence length is roughly consistent with the enhanced quasiparticle mass and consequently low Fermi velocity indicated by the high Sommerfeld coefficient of the specific heat capacity: we estimate the BCS coherence length from  $\xi_0 = (\hbar v_F)/(\pi\Delta)$  [7, 8], where  $v_F$  is the Fermi velocity and  $\Delta$  is the superconducting gap, approximated as  $1.76 k_B T_c$ . Representing the electronic structure of  $\text{YFe}_2\text{Ge}_2$  by one or two spherical Fermi surface sheets with radius  $k_F = 0.7 \text{ \AA}^{-1}$  (corresponding to half-filled bands) in order to extract  $v_F$  from  $\gamma$ , we would expect  $\xi_0 \simeq 130 \text{ \AA}$  for a single sheet or  $260 \text{ \AA}$  for two sheets. The mean free path in our samples can likewise be estimated (e.g. [8]) from  $\ell \simeq 1200 \text{ \AA} (\text{\AA}^{-2}/k_F^2)(\mu\Omega\text{cm}/\rho_0)$ , where  $\rho_0$  is the residual resistivity, to be about  $800 \text{ \AA}$  ( $400 \text{ \AA}$ ) for the highest quality samples, when one (two) Fermi surface sheets are assumed. This would indicate that  $\ell$  indeed exceeds  $\xi_0$ , so that anisotropic order parameters are not ruled out by disorder scattering.

Our findings suggest that  $\text{YFe}_2\text{Ge}_2$  may be sufficiently close to a quantum critical point to display signatures of Fermi liquid breakdown at ambient pressure. The observation of spin density wave order in the related material  $\text{LuFe}_2\text{Ge}_2$ , which is isoelectronic to  $\text{YFe}_2\text{Ge}_2$  but has a smaller unit cell volume, suggests that applied hydrostatic pressure may drive  $\text{YFe}_2\text{Ge}_2$  into a magnetically ordered state. High pressure studies are under way to

examine the evolution of the anomalous normal state and of the associated superconducting transitions in  $\text{YFe}_2\text{Ge}_2$  on approaching the presumed high pressure spin density wave critical point.

We thank C. Geibel, P. Niklowitz, S. Friedemann and G. G. Lonzarich for helpful discussions. This work was supported by EPSRC UK and Trinity College Cambridge.

---

\* Present address: London Centre of Nanotechnology, University College London, Gordon Street, London WC1H 0AH, UK

- [1] M. Avila, S. Bud'ko, and P. Canfield, *Journal of Magnetism and Magnetic Materials* **270**, 51 (2004).
- [2] J. Ferstl, H. Rosner, and C. Geibel, *Physica B: Condensed Matter* **378-380**, 744 (2006).
- [3] T. Fujiwara, N. Aso, H. Yamamoto, M. Hedo, Y. Saiga, M. Nishi, Y. Uwatoko, and K. Hirota, *Journal of the Physical Society of Japan* **76**, 60 (2007).
- [4] S. Ran, S. L. Budko, and P. C. Canfield, *Philosophical Magazine* **91**, 4388 (2011).
- [5] P. Blaha, K. Schwarz, G. Madsen, D. Kvasnicka, and J. Luitz, *WIEN2k User's Guide*, Vol. 1 (2013).
- [6] E. Helfand and N. R. Werthamer, *Phys. Rev.* **147**, 288 (1966).
- [7] M. Tinkham, *Introduction to Superconductivity*, Vol. 1 (Dover Publications, 2004).
- [8] T. P. Orlando, E. J. McNiff, S. Foner, and M. R. Beasley, *Phys. Rev. B* **19**, 4545 (1979).